DOI: 10.1002/anie.201206065

Electron Density

Pushing X-ray Electron Densities to the Limit: Thermoelectric $CoSb_3$**

*Mette Stokkebro Schmøkel, Lasse Bjerg, Jacob Overgaard, Finn Krebs Larsen, Georg Kent Hellerup Madsen, Kunihisa Sugimoto, Masaki Takata, and Bo Brummerstedt Iversen**

For more than three decades, electron densities (ED) have been determined in numerous crystals based on modeling of accurate structure factors measured by X-ray diffraction.[1] Today, the X-ray ED method is well established and has provided highly important insight into the nature of chemical bonding and physical properties of systems that span from small organic molecules to inorganic crystals and even proteins.[2–6] The complexity of the crystalline systems that are investigated with the X-ray ED method continue to increase, but the method has some fundamental limitations that have to be faced in all studies. Clearly, it is of interest to probe these limitations by testing the method in a "worst-case scenario".

$CoSb_3$ presents a great challenge for X-ray ED analysis. The structure consists of heavy atoms, in which the valence electrons only weakly contribute to the diffracted intensities, thus making modeling of the aspherical features of the chemical bonds difficult. This limitation is reflected in the very low value of the so-called suitability factor, $S = V/(\Sigma_{i,\text{unit cell}} n_{\text{core},I})$, which is approximately 0.013 for $CoSb_3$ versus typical values of around 5–10 for organic compounds.[7] Another point is the high symmetry and relatively small unit cell of the structure (≈ 9.02 Å). These factors make data modeling difficult, because there will only be relatively few non-equivalent low-order reflections that carry the majority of information on valence electrons. Furthermore, in highly crystalline inorganic solids, such as $CoSb_3$, these low-order reflections may be significantly affected by extinction, which can be difficult to account for. This problem has been addressed by Jauch and Reehuis in a range of γ-ray diffraction studies on inorganic compounds containing first-row transition elements. The high energy of γ-rays facilitates the collection of data at a very high resolution and with very little extinction.[8] A further complication related to $CoSb_3$ is the tendency for errors to accumulate at positions with high symmetry in high-symmetry structures.[9] Apart from extinction, systematic errors in X-ray data can originate from a variety of other sources, such as beam instability, absorption, integration errors etc.[10] Some of these effects can be significantly reduced by the combined use of small crystals and intense, high-energy, monochromatic synchrotron radiation.[11] Furthermore, systematic errors, such as thermal diffuse scattering (TDS) and anharmonicity, can be greatly reduced by collecting data at very low temperatures, which also enhances the intensity of the high-order reflections.[12]

For very simple structures, electron diffraction has been used to obtain accurate low-order structure factors,[13] but such studies are inherently limited to extremely simple compounds that are of limited interest in chemistry and materials science. In this context, $CoSb_3$ has a relatively large unit cell and, indeed, attempts to study the ED by electron diffraction have not been successful.[14] Our goal in the present study was to probe the level of accuracy that can be achieved for a challenging system such as $CoSb_3$, when using the most accurate data that can be measured currently (short-wavelength single-crystal synchrotron data at ≈ 10 K). The study is part of a large examination of various X-ray diffraction data sets that we measured on a wide range of conventional and synchrotron X-ray sources using different wavelengths and crystal sizes. These studies will be published elsewhere and focus on a range of technical issues. Here we communicate the main chemical findings based on the best data set and thereby provide an understanding of the current status of the X-ray ED method. The high symmetry and semimetallic properties of $CoSb_3$ make high-level DFT calculations accurate. Therefore, we can use theoretical structure factors as a benchmark for the quality of the experiment. To provide a direct comparison, both experimental and theoretical structure factors are refined with the multipole model,[15] because this avoids issues related to model bias.

$CoSb_3$ is an excellent system to probe the accuracy of the X-ray ED method, and it is also an important host–guest

[*] M. Stokkebro Schmøkel, L. Bjerg, Dr. J. Overgaard, Dr. F. Krebs Larsen, Prof. Dr. B. Brummerstedt Iversen
Center for Materials Crystallography, Department of Chemistry, and Interdisciplinary Nanoscience Center (iNANO), Aarhus University
Langelandsgade 140, 8000 Aarhus (Denmark)
E-mail: bo@chem.au.dk
Dr. G. K. Hellerup Madsen
Department of Atomistic Modelling and Simulation, ICAMS
Ruhr-Universität Bochum (Germany)
Dr. K. Sugimoto, Prof. Dr. M. Takata
Japan Synchrotron Radiation Research Institute
1-1-1, Kouto, Sayo-cho, Sayo-gun, Hyogo 679-5198 (Japan)

[**] This work was supported by the Danish National Research Foundation (Center for Materials Crystallography), the Danish Strategic Research Council (Center for Energy Materials), and the Danish Research Council for Nature and Universe (Danscatt). The synchrotron radiation experiment at the SPring-8 synchrotron was conducted with the approval of the Japan Synchrotron Radiation Research Institute.

Supporting information for this article is available on the WWW under http://dx.doi.org/10.1002/anie.201206065.

material to engineer high-performance thermoelectric materials.[16] $CoSb_3$ crystallizes in the cubic space group $Im\bar{3}$ ($Z = 8$), and one common way to look at the structure is in terms of trigonally distorted corner-sharing $CoSb_6$ octahedra connected by the Sb_4 rings (Figure 1 a). All Co–Sb interactions in the structure are equivalent, whereas there are two distinct

Figure 1. Structure of $CoSb_3$ depicting the $CoSb_6$ octahedra and the Sb_4 unit (a), and the 20-atom cages emphasizing the covalent-bonding description (b).

Sb–Sb interactions, resulting in two different interatomic bond lengths. Ohno et al. pointed out that the structure consists of large pentagonal dodecahedral cages centered around the (0,0,0) site in the unit cell (Figure 1 b).[17] These cages are linked by the longer Sb–Sb bonds, while the shorter Sb–Sb bonds form some of the edges in the cage, and Co–Sb bonds form the others. Upon doping, guest atoms can enter into the cages, and thereby lower the thermal conductivity of the compound.[18]

The static deformation density obtained from both experiment and theory (Figure 2) leads to the same qualitative result. Thus, charge is moved from the part of the antimony atoms pointing away from the ring to the Sb–Sb interatomic regions. In the experimental plot, the positive region of the deformation density is displaced slightly outward for the vertical, short Sb–Sb interaction, thus indicating the presence of a bent bond. The deformation density of the $CoSb_6$ octahedron shows maxima that point toward the faces of the octahedron, and minima that point toward the six ligands. In addition, positive deformation density is found in the Co–Sb interatomic region, thus indicating that the interaction also has some degree of covalency (see the Supporting Information). In terms of the Laplacian, the Co atom has eight valence shell charge concentrations pointing away from the ligands, in agreement with the deformation density around Co. These features reveal the local ED of the Co 3d electrons and are typical indicators of filled t_{2g} and unfilled e_g orbitals in an octahedral field.[15,19]

The topological descriptors at the bond critical points (bcp) are listed in Table 1.[20] Rather low values of ρ and $\nabla^2\rho$ are found, as expected for heavy atoms with diffuse valence densities, but the values of ρ_{bcp} and $\nabla^2\rho_{bcp}$ alone are not good indicators of the strength and nature of the interactions.[19,21] Instead, the covalent character of all bonds is confirmed by the negative value of the total energy density, H, and the finding that $G/\rho < 1$ for all interactions.[22] The value of G/ρ is higher for the Co–Sb bond, which may indicate a slightly more polar interaction. This assumption is supported by the fact that the atoms are slightly charged. When calculating the charges from integrations over the atomic basins (Table 2), the Co atom is negatively and the Sb atom positively charged, in fair agreement with the refined multipole populations. This observation is also made for the charges obtained directly

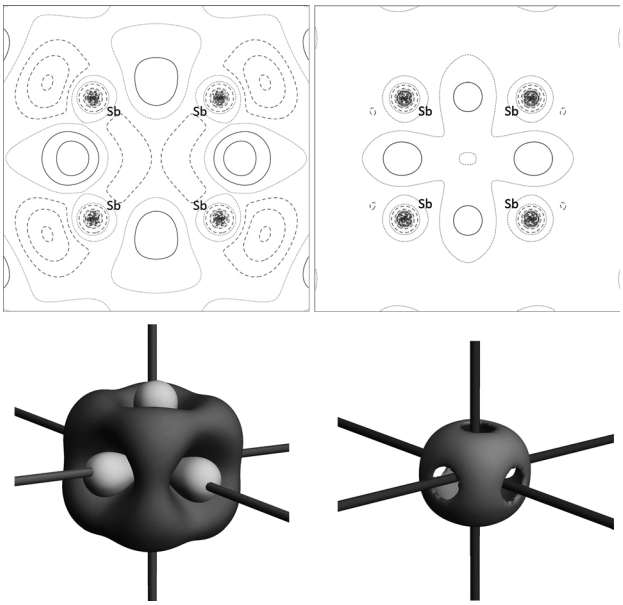

Figure 2. Static deformation density in the plane of the Sb_4 ring from multipole modeling of experimental structure factors (a) and theoretical structure factors (b) with a contour level of ± 0.05 e Å^3 (dark-gray: positive, light-gray: zero, dotted: negative). c) Static deformation density isosurface (± 0.25 e Å^3) of the $CoSb_6$ octahedra for the experimental data. Straight lines represent the directions toward Sb. d) 3D experimental Laplacian distribution of Co at a contour level of -700 e Å^5. For c and d, the corresponding plots from theory are shown in the Supporting Information.

Table 1: Topological analysis of the bond critical points ($\mathbf{r}_{bcp}$) in $CoSb_3$. d is the bond distance and AIL is the length of the atomic interaction line. ρ and $\nabla^2\rho$ are the electron density and its Laplacian, respectively. H, V, G/ρ are local total, potential, and normalized kinetic energy densities, respectively, in atomic units.

		Sb-Sb_{long}	Sb-Sb_{short}	Co-Sb
d [Å]	experim.	2.973	2.848	2.524
	theor.	2.973	2.848	2.524
$AIL_{Sb\text{-}x}$ [Å]	experim.	2.986	2.884	2.524
	theor.	2.973	2.848	2.524
$AIL_{Sb\text{-}bcp}$ [Å]	experim.	1.493	1.442	1.331
	theor.	1.486	1.424	1.343
$\rho(\mathbf{r}_{bcp})$ [e Å^{-3}]	experim.	0.330	0.402	0.395
	theor.	0.316	0.378	0.426
$\nabla^2\rho\ (\mathbf{r}_{bcp})$ [e Å^{-5}]	experim.	0.21	0.20	1.71
	theor.	0.33	0.17	1.54
$G(\mathbf{r}_{bcp})/\rho(\mathbf{r}_{bcp})$	experim.	0.42	0.46	0.64
	theor.	0.42	0.44	0.62
$V(\mathbf{r}_{bcp})$	experim.	−0.258	−0.357	−0.382
	theor.	−0.243	−0.322	−0.424
$H(\mathbf{r}_{bcp})$	experim.	−0.122	−0.171	−0.131
	theor.	−0.110	−0.155	−0.158

Table 2: Atomic basin integrations of Co and Sb in a.u. Q is the atomic charge, V the atomic basin volume, and μ the magnitude of the atomic dipole moment. The Lagrangian, $L = -1/4 \int_{\Omega} \nabla^2 \rho d\tau$, is a measure of the accuracy of the numerical integration of the atomic basin Ω.[15b]

		Co	Sb
Q_{QTAIM}	experim.	−0.63	0.22
	theor.	−0.49	0.18
V_{TOT}	experim.	99.53	173.22
	theor.	100.04	173.04
μ	experim.	0.01	0.66
	theor.	0.03	0.16
L	experim.	2.41×10^{-3}	1.67×10^{-1}
	theor.	1.13×10^{-3}	1.67×10^{-1}

from integration of the theoretical ED (i.e., without multipole modeling), which are −0.38 e for Co and 0.12 e for Sb.

The experimentally and theoretically obtained topology of the ED agree well with one another, and the same qualitative picture is obtained for all three types of bonds with relatively low values of ρ_{bcp}, but with clear indication of charge accumulation and shared-shell interactions. The most important general observation from the ED analysis is probably the fact that the Co atom carries a small negative charge (≈ -0.5), whereas the Sb atoms have a slight positive charge ($\approx +1/6$). This result contradicts a large part of the literature on thermoelectrics of skutterudites, but agrees well with the similarity in the electronegativities of the two elements. There has been discussion about whether ED-based methods, such as the quantum theory of atoms in molecules, can bring any real insight into chemistry when compared with orbital-based methods. In the present case, the orbital-based analyses give a different interpretation of the charge flow in $CoSb_3$ to that found by experimental observations.[23–25] The ED analysis indicates that the Co–Sb and Sb–Sb interactions are qualitatively similar in character, and that the structure can be viewed as consisting of pyritohedral cages connected by long Sb–Sb atomic interactions (Figure 1b).

Because $CoSb_3$ is known to be a low-spin, diamagnetic, and semiconducting compound, speculations on the population of the 3d orbitals can be made.[26,27] In the simple picture given by, for example, Grosvenor et al., the nonmagnetic behavior of Co is explained for an undistorted octahedral d-splitting by the loss of the two 4s and one 3d electron, leading to a paired-spin $3d^6$ configuration.[24] The preferentially filled low-energy t_{2g} orbitals dominate the Laplacian distribution of the Co atom and there are no clear indications of density features from the high-energy e_g density. However, the negative charge of the Co atom and the covalent character of the Co–Sb bond tell another story. These features are indications of the presence of some degree of mixing between the e_g orbitals on Co and the 5s5p valence on Sb. The diamagnetic, semiconducting properties of the compound can possibly be explained with filled t_{2g} orbitals, and e_g electrons participating in bonding through 3d-5p-hybridized orbitals between Co and Sb, as suggested by Dudkin in 1958[28] and later confirmed in various other studies.[24,29] Another view could be to assume that Co has a charge of −1 and that the 4s electrons are placed in the d-shell. This would lead to a closed-shell diamagnetic d^{10} ion. However, this assumption is in clear contradiction with the nonspherical Laplacian distribution.

The nature of the chemical bonding in $CoSb_3$ has an impact on the understanding of the thermoelectric properties. In numerous reports, it is assumed that guest atoms occupy the cubic space formed by eight Co^{3+} ions, and the key mechanism for lowering the thermal conductivity is so-called rattling behavior, in which the guest atom exhibits low-energy thermal vibration in an oversized cavity.[14] Thus, the crucial point is to understand the potential in which the guest atom is placed. In order for the guest atom to lower the thermal conductivity, it must interact with the host system, a process often coined "coupling". Clearly, this coupling is different in nature if the guest atom is placed in a 20-atom cage consisting of covalently linked Co and Sb atoms with relatively low charge rather than a highly charged cage consisting of eight Co^{3+} cations. The present study shows that the ionic picture of $CoSb_3$ is incorrect, and future studies of skutterudites should interpret their results within the covalent bonding model.

Overall, the present study provides an encouraging view of the current accuracy of the X-ray ED method. Provided that utmost care is taken then highly accurate EDs can be obtained even in the most unfavorable cases such as $CoSb_3$.

Experimental Section

Data collection: Single-crystal X-ray diffraction data (10 K) were collected on a single crystal (≈ 10 μm) using a wavelength of 0.4117 Å at the BL02B1 beamline at SPring8, Japan. The beamline was equipped with a Rigaku 1/4 chi goniometer and a cylindrical image plate detector. Data were collected to $\sin\theta/\lambda_{max} = 1.67$ Å^{-1} resulting in 58020 reflections of which 2559 are unique. The agreement of equivalents before correction of the data was $R_{int}(I) = 0.046$, and after $R_{int}(I) = 0.038$. Empirical absorption ($T_{min} = 0.931$, $T_{max} = 1.055$) and oblique incidence corrections were carried out with ABSCOR.[30]

Theoretical calculations: The electron density of $CoSb_3$ was determined in the experimental geometry by DFT calculations using the *WIEN2k* package.[31] Structure factors were obtained by Fourier transformation of the theoretical density. Calculations were done using the PBE functional on an $11 \times 11 \times 11$ k grid with $RK_{max} = 10$. The charge density within the atomic spheres was expanded to include spherical harmonics up to $L = 10$.

Multipole modeling: Experimental and theoretical structure factors with $\sin\theta/\lambda < 1.6$ Å^{-1} were refined against the Hansen-Coppens multipole model in the program *XD2006*.[11] Aspherical atom models employing scattering factors derived from STO relativistic wave functions (the *VM* data bank) were used. Multipolar functions up to hexadecapole level were refined for both atoms. For the theoretical structure factors, all positional parameters were kept fixed in the experimental geometry, and the radial coefficients (κ, κ') were allowed to vary freely. For the experimental data refinement ($I > 3\sigma(I)$), the scale factor, atomic positions, and anisotropic displacement parameters were refined, whereas κ and κ' were held fixed at the values determined from modeling of the theoretical structure factors. Because of the problem of simultaneously treating the 4s and 3d shells as valence for transition-metal elements, only the 3d shell on Co was considered as valence while the 4s shell was considered as part of the core density.[32] When treating the 4s electrons as a separate valence shell, the valence population of this shell refined to values close to 2 in support of the approach described above (see the Supporting Information). Irrespective of the treatment of the Co valence density in the modeling, the 3d population refined to values slightly above 7 electrons. An isotropic, type I extinction

correction with a Lorentzian mosaic distribution[33] was included in the refinement, and excellent refinement residuals were obtained with ($R(F) = 0.03\,\%$ for theory and $R(F^2) = 1.27\,\%$ for experiment. Further description of the multipole modeling is given in the supporting information.

Received: July 29, 2012
Revised: October 10, 2012
Published online: December 13, 2012

Keywords: electron density · low-temperature physics · skutterudites · thermoelectric materials · X-ray diffraction

[1] P. Coppens, *X-ray charge densities and chemical bonding*, Oxford University Press, New York, **1997**.
[2] T. S. Koritsanszky, P. Coppens, *Chem. Rev.* **2001**, *101*, 1583.
[3] P. Coppens, B. B. Iversen, F. K. Larsen, *Coord. Chem. Rev.* **2005**, *249*, 179 – 195.
[4] C. Gatti, P. Macchi, *Modern Charge Density Analysis*, Springer, Heidelberg, **2012**.
[5] D. Stalke, *Electron Density and Chemical Bonding I* (Experimental) and *II* (Theoretical) in *Structure and Bonding*, Springer, Berlin, **2012**.
[6] a) D. Housset, F. Benabicha, V. Pichon-Pesme, C. Jelsch, A. Maierhofer, S. David, J. C. Fontecilla-Camps, C. Lecomte, *Acta Crystallogr. Sect. D* **2000**, *56*, 151 – 160; b) C. Lecomte, E. Aubert, V. Legrand, F. Porcher, S. Pillet, B. Guillot, C. Jelsch, *Z. Kristallogr.* **2005**, *220*, 373 – 384.
[7] E. D. Stevens, P. Coppens, *Acta Crystallogr. Sect. A* **1976**, *32*, 915 – 917.
[8] a) W. Jauch, M. Reehuis, *Phys. Rev. B* **2002**, *65*, 125111; b) W. Jauch, M. Reehuis, *Phys. Rev. B* **2009**, *80*, 125126.
[9] B. Rees, *Acta Crystallogr. Sect. A* **1976**, *32*, 483 – 488.
[10] B. B. Iversen, F. K. Larsen, B. N. Figgis, P. A. Reynolds, A. J. Schultz, *Acta Crystallogr. Sect. B* **1996**, *52*, 923 – 932.
[11] a) B. B. Iversen, F. K. Larsen, A. A. Pinkerton, A. Martin, A. Darovsky, P. A. Reynolds, *Acta Crystallogr. Sect. B* **1999**, *55*, 363 – 374; b) J. Overgaard, B. Schiøtt, F. K. Larsen, A. J. Schultz, J. C. Macdonald, B. B. Iversen, *Angew. Chem.* **1999**, *111*, 1321 – 1324; *Angew. Chem. Int. Ed.* **1999**, *38*, 1239 – 1242.
[12] F. K. Larsen, *Acta Crystallogr. Sect. B* **1995**, *51*, 468 – 482.
[13] J. M. Zuo, M. Kim, M. O'Keeffe, J. C. H. Spence, *Nature* **1999**, *401*, 49 – 52.
[14] R. Sæterli, E. Flage-Larsen, J. Friis, O. M. Løvvik, J. Pacaud, K. Marthinsen, R. Holmestad, *Ultramicroscopy* **2011**, *111*, 847 – 853.
[15] a) N. K. Hansen, P. Coppens, *Acta Crystallogr. Sect. A* **1978**, *34*, 909 – 921; b) XD2006—A Computer Program Package for Multipole Refinement, Topological Analysis of Charge Densities and Evaluation of Intermolecular Energies from Experimental or Theoretical Structure Factors, A. Volkov, P. Macchi, L. J. Farrugia, C. Gatti, P. Mallinson, T. Richter, T. Koritsanszky, **2006**.
[16] D. T. Morelli, T. Caillat, J.-P. Fleurial, A. Borshchevsky, J. Vandersande, B. Chen, C. Uher, *Phys. Rev. B* **1995**, *51*, 9622 – 9628.
[17] A. Ohno, S. Sasaki, E. Nishibori, S. Aoyagi, M. Sakata, B. B. Iversen, *Phys. Rev. B* **2007**, *76*, 064119.
[18] B. C. Sales, D. Mandrus, R. K. Williams, *Science* **1996**, *272*, 1325 – 1328.
[19] C. Gatti, *Z. Kristallogr.* **2005**, *220*, 399 – 457.
[20] R. F. W. Bader, *Atoms in Molecules: A Quantum Theory*, Clarendon, Oxford, **1990**.
[21] P. Macchi, A. Sironi, *Coord. Chem. Rev.* **2003**, *238 – 239*, 383 – 412.
[22] Y. A. Abramov, *Acta Crystallogr. Sect. A* **1997**, *53*, 264 – 272.
[23] D. Jung, M.-H. Whangbo, S. Alvarez, *Inorg. Chem.* **1990**, *29*, 2252.
[24] A. P. Grosvenor, R. G. Cavell, A. Mar, *Phys. Rev. B* **2006**, *74*, 125102.
[25] G. A. Papoian, R. Hoffmann, *Angew. Chem.* **2000**, *112*, 2500; *Angew. Chem. Int. Ed.* **2000**, *39*, 2408.
[26] H. Anno, K. Matsubara, T. Caillat, J.-P. Fleurial, *Phys. Rev. B* **2000**, *62*, 10737 – 10743.
[27] a) J. Yang, G. P. Meisner, D. T. Morelli, C. Uher, *Phys. Rev. B* **2001**, *63*, 014410; b) K. Koga, K. Akai, K. Oshiro, M. Matsuura, *Phys. Rev. B* **2005**, *71*, 155119.
[28] L. D. Dudkin, *Sov. Phys. Techn. Phys.* **1958**, *3*, 216.
[29] a) D. J. Singh, W. E. Pickett, *Phys. Rev. B* **1994**, *50*, 11235 – 11238; b) I. Lefebvre-Devos, M. Lassalle, X. Wallart, J. Olivier-Fourcade, L. R. Monconduit, J. C. Jumas, *Phys. Rev. B* **2001**, *63*, 125110; c) H. Ishii, K. Okazaki, A. Fujimori, Y. Nagamoto, T. Koyanagi, J. O. Sofo, *J. Phys. Soc. Jpn.* **2002**, *71*, 2271 – 2275.
[30] Rigaku, ABSCOR, Rigaku Corporation, Tokyo, Japan, **1995**.
[31] P. Blaha, K. Schwarz, G. Madsen, D. Kvasnicka, J. Luitz, WIEN2k, Techn. Universität Wien, **2008**.
[32] L. J. Farrugia, P. R. Mallinson, B. Stewart, *Acta Crystallogr. Sect. A* **2003**, *59*, 234 – 247.
[33] P. J. Becker, P. Coppens, *Acta Crystallogr. Sect. A* **1974**, *30*, 129 – 147; P. J. Becker, P. Coppens, *Acta Crystallogr. Sect. A* **1974**, *30*, 148 – 153.

